Applied Catalysis B: Environmental 96 (2010) 1–9

Contents lists available at ScienceDirect

Applied Catalysis B: Environmental

journal homepage: www.elsevier.com/locate/apcatb

Partial oxidation of ethanol over cobalt oxide based cordierite monolith catalyst

Clarissa Perdomo Rodrigues, Victor Teixeira da Silva, Martin Schmal *

NUCAT/PEQ/COPPE, Federal University of Rio de Janeiro, C.P. 68502, 21945-970, Rio de Janeiro, Brazil

ARTICLE INFO

Article history:
Received 1 September 2009
Received in revised form 20 January 2010
Accepted 26 January 2010
Available online 2 February 2010

Keywords:
Monolithic catalysts
Structured catalysts
Ethanol partial oxidation

ABSTRACT

Ethanol partial oxidation was studied on Co_3O_4/γ–Al_2O_3/cordierite honeycomb structured catalyst. Honeycomb structure consists of parallel channels that favor the gas phase reactions, which in some temperature and flow rate conditions could be limited by mass transfer effects in gas phase. The catalytic activity and products selectivity were evaluated at different temperatures and O_2:ethanol ratios. Also, it evaluated the effect of space velocity (h^{-1}) and presence of H_2O in the feed. Overall, the results showed that the partial oxidation reaction occurs in a way that the ethanol is first decomposed in gas phase and then formed in the presence of oxygen radicals that decomposed on the catalyst surface. The CO_2:CO low ratio observed in most experiments indicates that shift reaction occurs in gas phase and its equilibrium limits the hydrogen formation. Although this catalyst has not presented any significant deactivation, some carbon formation was observed after 30 h on reaction.

1. Introduction

During the 1990s, there was an increasing interest in producing cheaper synthetic fuels, and the catalytic partial oxidation became widely studied in the industries and academic research groups [1–7]. In most laboratory research, the partial oxidation studies were done in fixed bed microreactors. These reactors present disadvantages such as sintering, pressure drop and preferential path toward the bed.

A promising alternative to eliminate the disadvantages of fixed bed reactor is the monolithic reactor [8]. The advantage in developing processes using monolith-based reactors is the extremely low contact time (in the order of milliseconds). Olefins production via catalytic oxidative dehydrogenation of light paraffin and hydrogen production via catalytic partial oxidation of hydrocarbons are the most important processes for which applications of monolithic catalysts have been evaluated [9].

In general, the temperature for partial oxidation is extremely high at very low contact time that corresponds to space velocities range from 2 to 1×10^5 h^{-1} where different products are involved and different mechanistic conclusions are drawn [10–13].

Besides, the literature [11,14] shows that at higher temperatures and space velocities the surface and gas film reactions are favored, resulting in a mass transfer limited process inside the individual monolith passages. An alternative to minimize the effects of mass transfer is to use catalysts preparation methodologies that reduce the cross-sectional area in contact with reagent flow and concentrate the active sites of the catalyst on the surface of the monolith channel. In this case, the washcoating method in two stages showed evidences that it is the best option to minimize the cross-sectional area of monolith channels [13]. Another alternative is to improve the operating conditions in order to promote the formation of H_2 and inhibit the effects of mass transfer in gas phase.

Although the catalytic partial oxidation process to produce hydrogen has never been used commercially, it is the most promising because it offers advantages as low operation temperatures and low formation of soot or secondary products. Another important aspect of the partial oxidation is the space velocity at which the reactors operate, that is able to provide a negligible pressure drop in the packed bed reactor. According to Hohn and Schmidt [5] studies on the methane partial oxidation showed that the use of high space velocity results in a decrease of conversion and selectivity. Therefore, the oxidation of light hydrocarbons on monolithic reactors with low contact time has been intensively studied, showing satisfactory results with regard to conversion, selectivity to synthesis gas, operating conditions, no formation of carbon and reactor dimensions.

The literature is very scarce on information about the partial oxidation of ethanol. However, some authors [10–14] have reported that it is possible to produce hydrogen directly from ethanol by the reaction shown in Eq. (1). The subscripts *s* and *g* in the Eq. (1) mean respectively *steam* and *gas phase*. This reaction can be seen as a promising procedure to produce hydrogen because it offers advantages as rapid ignition and size of reactor. In this case, the reactor used is more compact than the system required to

* Corresponding author. Tel.: +5521 2562 8352; fax: +5521 2562 8300.
E-mail address: schmal@peq.coppe.ufrj.br (M. Schmal).

0926-3373/$ – see front matter © 2010 Elsevier B.V. All rights reserved.
doi:10.1016/j.apcatb.2010.01.027

perform steam reforming, because it does not require the addition of indirect heat.

$$C_2H_5OH_{(s)} + {}^1/_2O_2 \rightarrow 2CO_{(g)} + 3H_2(g) \quad (1)$$

The use of ethanol for the production of synthesis gas has some advantages such as it is easy to store and to transport because reactions occur at low temperatures. Producing hydrogen from ethanol results in low greenhouse gases emission, since the CO_2 produced in this process is consumed by the plantations of sugar cane during photosynthesis. The experience in the production and usage of ethanol comes from the 1980s, when alcohol was used as fuel in automotive vehicles or as an additive in gasoline [15].

The production of hydrogen on catalysts, such as nickel, cobalt, copper, chromium and noble metals supported on metal oxide, using an ethanol-water mixture as reagent, and systems in powder, pellets or foam ceramic are reported in the literature [10–18]. The main advantage in adding water to ethanol is to favor reforming reactions that maximize H_2 production and minimize CO in an exothermic process [14].

The product distribution is influenced by reaction temperature and the nature of the metal-based catalyst. At low temperatures, Ru and Pd catalysts produced mainly acetaldehyde and water. In other hand, at temperatures above 500 °C the conversion of ethanol is complete, with formation of decomposition products. Moreover, in most cases they were evaluated at temperatures above 700 °C, with the formation of H_2, CO and traces of CH_4 favored by reforming reactions.

Cobalt is presented in the literature [19–22] as a promising metal for hydrogen production from ethanol, owing to its ability to break ethanol C–C bonds and inhibit CH_4 formation from CO. When supported on Al_2O_3, cobalt (about 8 wt.%) can inhibit acidic properties of the support, which are responsible for promoting ethanol dehydration reaction.

Therefore, the main objective of this work is to study the ethanol partial oxidation reaction in a monolithic reactor taking as the main parameter the residence time that may avoid parallel and secondary reactions. The contact time selected is usually of the order of 0.2 s, which corresponds to a space velocity about $1{,}2 \times 10^4\ h^{-1}$ at temperatures between 260 and 770 °C. A cobalt-alumina washcoating on a honeycomb monolith was prepared for the partial oxidation of ethanol.

2. Experimental

2.1. Catalyst preparation

The honeycomb cordierite monolithic presents a cell density of 400 cells in^{-2} (D = 12 mm, L = 8 mm) and the catalyst was prepared by washcoating γ-alumina and cobalt as active phase. The γ-alumina support was prepared using a transition alumina solution using the urea method described elsewhere [23].

Several pieces of cordierite monoliths were dipcoated simultaneously in an acidic slurry of transition alumina with 1 wt.% EKASOL (EKA Chemicals Brazil S./A.) as a binder and allowed to soak for 4 days under continuous stirring. After dipcoating, the excess solution was drained with air blowing. The pieces were then subsequently dried at 200 °C for 120 min and calcined in air for 300 min at 500 °C. The dipcoating cycles finished when the fixed amount of washcoated reached 10 wt.% of γ-Al_2O_3.

The active phase was added with an aqueous solution of cobalt nitrate (Co $(NO_3)_2{\cdot}6H_2O$, VETEC), with a cobalt concentration of 291 g L^{-1}. The catalyst was then dried at 200 °C for 120 min and calcined in air for 120 min at 500 °C. The monoliths were repeatedly dipped, dried and calcined until cobalt loading reached 6 wt.% of the washcoating.

2.2. Catalyst characterization

The coating adherence was qualitatively measured by ultrasonic vibration test according to the method described elsewhere [24,25]. After each 30 min, the sample was dried and the weight loss measured.

Ethanol temperature-programmed desorption measurements were carried out using a flow system coupled to a quadrupole mass spectrometer (Balzers Prisma-QMS200). The sample was reduced at 500 °C in a mixture of 2% H_2 in helium flow. Ethanol was introduced using a saturator with helium carrier gas at room temperature. TPD of ethanol was performed at 20 °C min^{-1} from RT up to 500 °C under helium flow (30 mL min^{-1}).

At the end of evaluation tests, Co_3O_4/γ–Al_2O_3/cordierite catalyst was studied by Raman spectroscopy at RT using a Horiba Jobin Yvon Labra HR800 spectrometer equipped with a CCD detector and He-Ne laser (633 nm) as a lighting source and laser power was limited to 1.7 nW to minimize warming effects. This technique was used to identify the presence of carbon deposits on the catalyst, which shows characteristics bands in the range 1150–1750 cm^{-1}. Scanning electron microscopy analysis in emission field (FEG-SEM) was performed in Quanta 200 microscope (FEI) with maximum operating voltage of 20 kV. The images were acquired using EDT detector. Details of operating conditions for images acquisition, such as spot size and working distance (WD), and sample region extension observed are available in the micrographic bar presented here.

To evaluate catalyst thermal behavior and its resistance for carbon formation it was performed simultaneous thermogravimetric analysis of catalyst after had been removed from the reactor. To perform these tests we used a Rigaku Thermoplus TG 8120 thermal analyzer with 70 mL min^{-1} ultra pure gas flow of nitrogen and 8 mL min^{-1} ultra pure gas flow of oxygen. Temperature range analyzed was from RT up to 1000 °C at a heating rate of 10 °C min^{-1}. X-ray diffraction analysis was performed to verify possible changes in the crystalline structure of the catalyst after reaction. The analysis was done using a Rigaku X-ray diffractometer equipped with UTLIMA$^+$ goniometer, by kα copper radiation, using powder methodology evaluating $5 \leq 2\theta \leq 100°$ range, speed of analysis of 0.02 with steps every 5 s.

2.3. Catalytic tests

The tests were performed to evaluate the Co_3O_4/γ–Al_2O_3/cordierite monolithic catalyst for the ethanol partial oxidation and the influence of the experimental conditions, such as temperature, O_2:ethanol molar ratio, H_2 addition in the reactant feed, space velocity and H_2O addition in the reactant feed. Furthermore, cordierite monolithic catalyst stability was evaluated through long time test.

The partial oxidation reaction of ethanol P. A. (Vetec) was performed in an experimental unit consisting of a set of mass flowmeters (MKS) and a reactor coupled to a resistive furnace. The liquid was pumped to a vaporizer heated at 180 °C and then mixed with the gas stream. The reactor consists of a U shape quartz microreactor with 12 mm ID and 250 mm long. The catalyst was supported by quartz wool.

After 60 min under reactions conditions the samples were analyzed by gas chromatography (Varian CP3800) equipped with a thermal conductivity detector (TCD) and a flame ionization detector (FID) with a methanizer. The effluent gas was analyzed on two packed columns (Poraplot Q and Carbosieve 5A) using N_2 as the carrier gas. Reaction gases are supplied from high-pressure gas cylinders (AGA) with high purity.

Contact time of gas flow and catalytic bed was defined as the inverse of gas hourly space velocity (GHSV). Gas hourly space

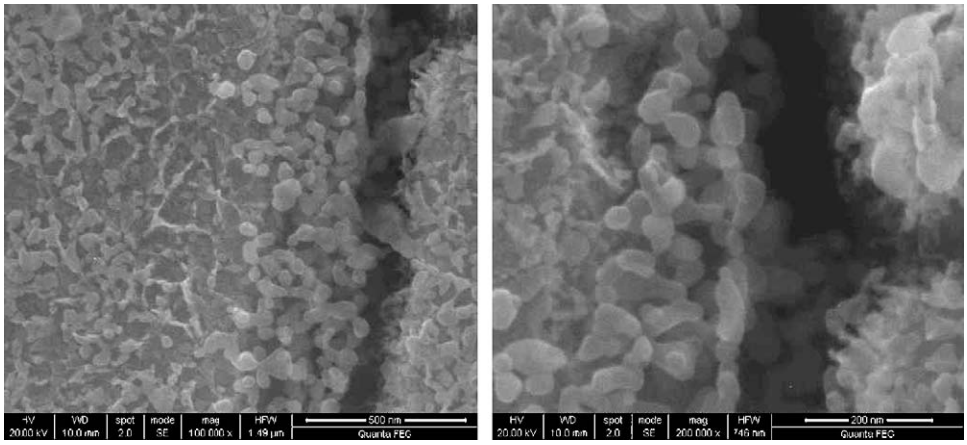

Fig. 1. SEM Images of Co_3O_4/γ–Al_2O_3/cordierite: 100 k and 200 k.

velocity was defined as the ratio of the volumetric flow of reactants at reaction conditions (420 °C and 1 atm) to the total catalyst volume as described elsewhere [11].

The products from partial oxidation reaction of ethanol detected by gas chromatography were hydrogen, methane, carbon dioxide, carbon monoxide, ethylene, ethane and acetaldehyde. Conversion of ethanol was calculated from carbon products molar balance, according to the definition described elsewhere [26]. The equation obtained to calculate the conversion of ethanol (on dry basis) is shown in Eq. (2), where γ_{Ci} is the ratio of carbon content in product *i* to carbon content in ethanol molecule and y_{Ci} is the molar fraction of carbon content products in effluent flow. Total product molar selectivity for ethanol partial oxidation reaction was defined as the ratio of moles of one product to total moles of products, based on experimental values.

$$X_{\text{Ethanol}}(\%) = \frac{\sum \gamma_{Ci} y_{Ci}}{y_{\text{Ethanol}} + \sum \gamma_{Ci} y_{Ci}} \times 100 \quad (2)$$

3. Results and discussions

3.1. Catalyst preparation and characterization

γ-Al_2O_3-coated cordierite monoliths prepared via an adapted version of urea method presented good washcoating adherence and dispersion of oxide phases, showing good reproducibility and similar experimental fluctuations assigned to cordierite losses during immersion step. The transition alumina precipitated on cordierite surface was evaluated by X-ray diffraction (XRD) and the result showed characteristic peaks of γ-phase alumina, commonly employed as catalytic support. Statistical analysis [27] for sample weight showed that the preparation methodology used presents high reproducibility with 98% ensuring. In addition, SEM images were taken to ensure that the catalyst was deposited over cordierite surface overall.

Co_3O_4/γ–Al_2O_3-coated cordierite monolith catalysts were 6.7 wt.% of metal oxide based on the total mass of the monolith support, after four cycles of immersion and heat treatment. SEM observations are presented in Fig. 1, which shows details of the particles deposited on the fissures of the support. The Co_3O_4/γ–Al_2O_3/cordierite mapping is presented in Fig. 2. From these results it is possible to say that the surface is principally composed by particles of alumina and cobalt. Energy dispersive X-ray spectroscopy signals showed in Fig. 2(g) confirm the presence of cobalt in the particles deposited at the surface of γ-Al_2O_3-coated cordierite. Besides that, the washcoating method in steps results in a good dispersion of γ-Al_2O_3 and Co_3O_4 over the cordierite surface.

The coating adherence was qualitatively measured by an ultrasonic vibration test. This test evaluated the weight loss by exposure to ultrasonic. The weight loss for γ-Al_2O_3 was 1.3% and for Co_3O_4 was 0.6% after exposure to ultrasonic vibration for 30 min, which are extremely good when compared to reported values in the literature, about 4.0% [19]. These results confirm that the urea method is efficient for washcoating γ-Al_2O_3 phase and cobalt-oxide over a cordierite monolith.

Fig. 3 shows the TPD profile after adsorption of ethanol on Co_3O_4/γ–Al_2O_3/cordierite. Ethanol desorbed at two temperatures centered at 140 and 280 °C. At lower temperature, there is CO, methane, acetaldehyde, ethylene and CO_2 desorption. Simultaneous peaks of CO, methane and CO_2 could be attributed to acetaldehyde and ethanol desorbed decompositions. At this temperature also starts H_2O desorption, suggesting that this catalyst favors dehydration reactions.

At 140 °C, a small desorption of acetic acid and acetone was observed by reason of dissociative adsorption with steam reforming (Eq. (3)) and ethanol decomposition (Eq. (4)). However, no ethane neither ethyl ether was detected. The subscripts *s*, *l* and *g* in the Eqs. (3) and (4) mean respectively *steam*, *liquid* and *gas phase*.

$$C_2H_5OH_{(s)} + H_2O_{(s)} \rightarrow CH_3COOH_{(l)} + 2H_{2(g)} \quad (3)$$

$$2C_2H_5OH_{(s)} \rightarrow CH_3COCH_{3(l)} + CO_{(g)} + 3H_{2(g)} \quad (4)$$

At 280 °C, the conditions for ethanol dehydrogenation reaction become favorable as a result of acetaldehyde presence and the beginning of H_2 desorption. H_2 appeared at 350 °C. At this temperature, there is also a simultaneous CO desorption, which suggests that the partial oxidation reaction of ethanol becomes favorable.

Similar results were found in the literature [28] on 7% Co–Al_2O_3 catalyst. These results showed that at low temperatures, between 122 and 187 °C, and ethanol–water mixture, the desorbed products were acetaldehyde, CO and methane. At 252 °C, peaks appeared from CO and methane, which are attributed to the decomposition of acetaldehyde and ethanol desorption.

At higher temperature, centered at 440 °C, CO_2 desorption and H_2 in lower intensity was observed, which could be attributed to ethanol steam reforming (Eq. (5)), since the intensity of H_2O peak showed a decrease that started at 350 °C. Furthermore, the CO_2 formation at this temperature could be attributed to the decomposition of acetyl group as suggested by Haga et al. [28].

$$C_2H_5OH_{(s)} + 3H_2O_{(s)} \rightarrow 2CO_{2(g)} + 6H_{2(g)} \quad (5)$$

The literature [15] reports that CO, methane and H_2 desorption occurred at temperature around 400 °C on Co–

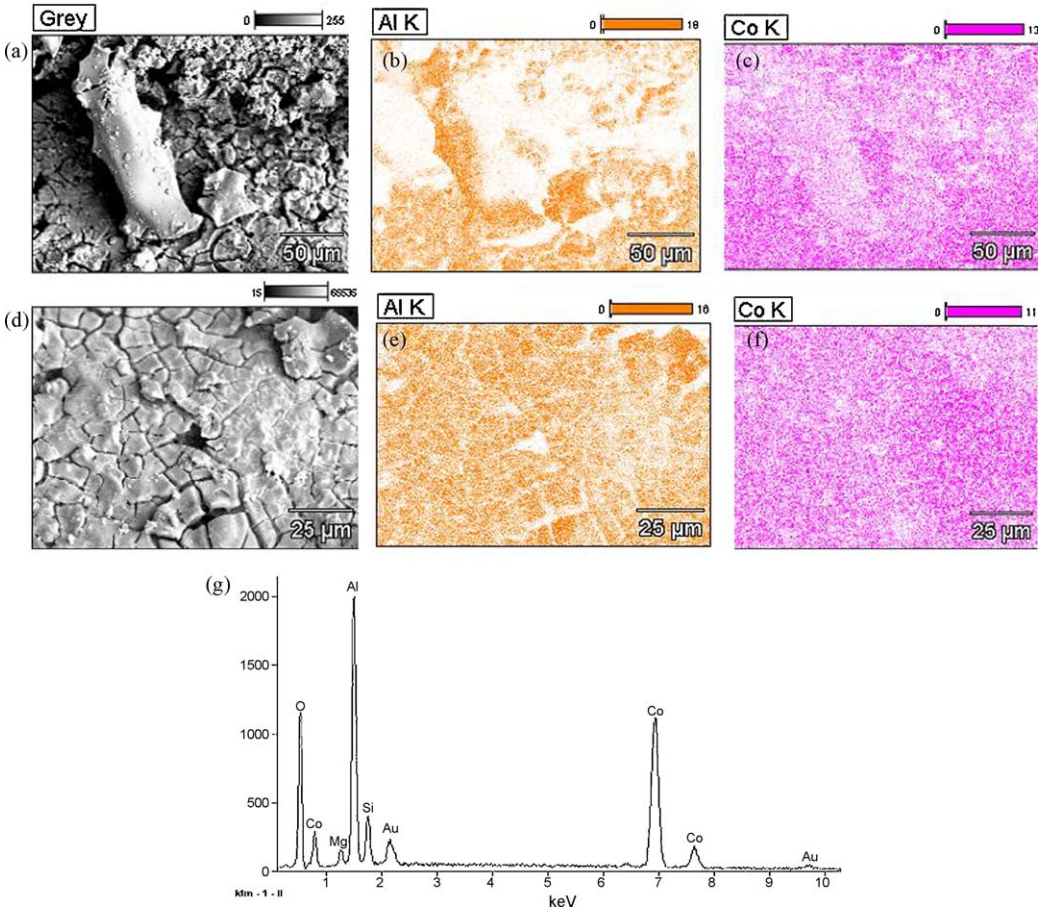

Fig. 2. Element mapping of alumina and cobalt and EDS measurements on Co_3O_4/γ–Al_2O_3/cordierite.

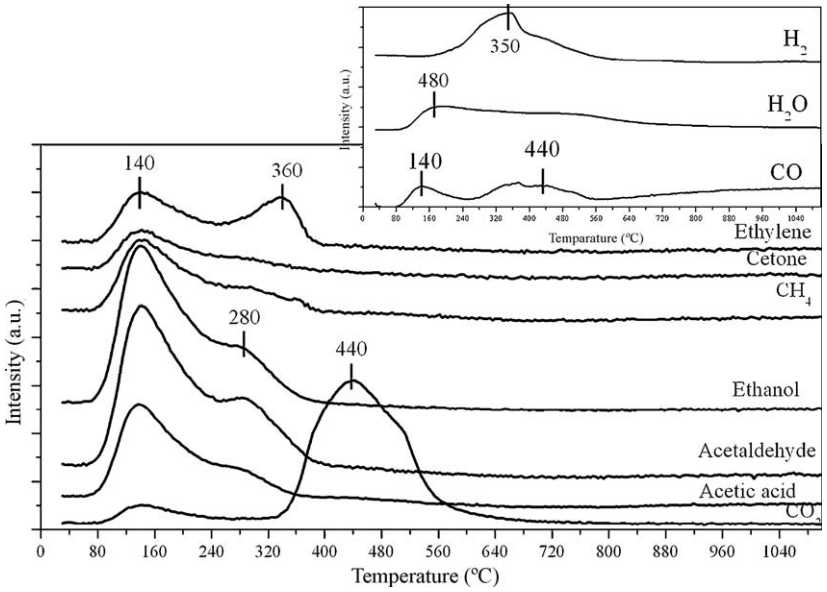

Fig. 3. TPD profiles of ethanol adsorbed on Co_3O_4/γ–Al_2O_3/cordierite.

CeO_2 catalyst surface. According to them, the formation of these species could be attributed to the decomposition of adsorbed ethoxy species, which occurred at higher temperatures on Co–CeO_2 catalyst. Furthermore, the formation of CO and CO_2, at 400 °C were observed, which could be attributed to a facile decomposition followed by an oxidation of acetate species resulting in a formation of carbonate species that underwent to decomposition.

In general, the Co_3O_4/γ–Al_2O_3/cordierite catalyst presents active sites for ethanol, ethylene and acetaldehyde decomposition to produce CO, methane and CO_2. These results confirm the capacity of cobalt breaking C–C bonds.

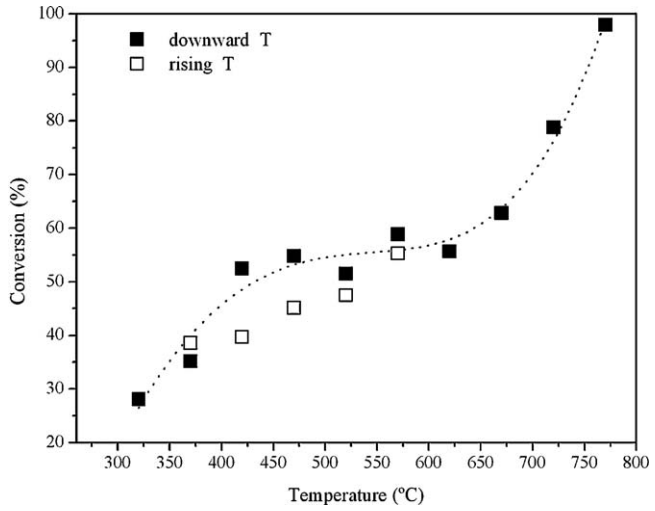

Fig. 4. Conversion of ethanol on partial oxidation as a function of reaction temperature at constant values of GHSV ($1.8 \times 10^4\ h^{-1}$) and O_2:ethanol (0.3).

Table 1
Response of CO_2:CO molar ratio and products distribution during partial oxidation of ethanol at low temperatures (GHSV = $1{,}8 \times 10^4\ h^{-1}$; O_2:ethanol = 0.3).

T (°C)	$X_{Ethanol}$ (%)	CO_2:CO (molar ratio)	Selectivity (mol.%)	
			Ethylene + ethyl ether + CO + CO_2	Acetaldehyde
320	28.1	4.4	26.7	82.6
370	35.2	3.3	23.6	74.7
420	52.5	0.4	44.1	50.3

3.2. Catalytic evaluations

3.2.1. Effect of reaction temperature

The effect of reaction temperature was studied in the range from 260 to 770 °C, with a total inlet flow of 200 mL min^{-1} and O_2:ethanol molar ratio of 0.3. The results are displayed in Fig. 4. Co_3O_4/γ–Al_2O_3/cordierite was evaluated in two ways: first a ramp from 370 up 570 °C, and second, after decreasing temperature to 320 °C, rising progressively to 770 °C. In Fig. 4, it is possible to observe a small difference among ethanol conversions in ascending and descending temperatures indicating that the catalyst undergoes to activation at the reaction conditions. The catalyst does not deactivate under reaction conditions and as reaction temperature increases. In addition, the ethanol conversion increases also. Total consumption of oxygen was observed above 420 °C.

The ethanol conversion started above 320 °C and total conversion was reached at 770 °C. According to the literature [29], a slightly lower conversion was obtained on the basis of H contents of ethanol introduced and products formed. The conversion of ethanol almost doubled between 320 and 420 °C as a result of the catalyst activation. The products detected were hydrogen, methane, carbon dioxide, carbon monoxide, ethylene, ethane and acetaldehyde, and these selectivities on a water-free basis are presented in Table 1. This table clearly shows that at lower temperatures, when the conversion of ethanol is about 30%, the products selectivities are high for dehydrogenation reaction products as acetaldehyde, ethylene and diethyl ether.

At 420 °C there was a considerable increase in the ethanol conversion, causing a modification in the products distribution and the activation of the catalyst. The CO_2:CO molar ratio decreased significantly suggesting that the reverse water–gas shift reaction (Eq. (6)) prevails, favoring the CO formation.

$$CO_{(g)} + H_2O_{(s)} \leftrightarrow CO_{2(g)} + H_{2(g)} \quad (6)$$

Contrary to the literature, one observed large amounts of acetaldehyde in this study. Sahoo et al. [20] showed some traces of acetaldehyde formation on Co–Al_2O_3 catalyst, about 0.05 to 0.1% (mole) at ethanol conversions of 10% and 40%. Moreover, these authors observed that over 40% no acetaldehyde was formed. This fact confirms that the dehydrogenation of ethanol to form acetaldehyde may occur in the gas phase, under the experimental conditions employed in the present study.

At high temperatures (520 °C to 770 °C) ethanol conversion remained approximately constant until 670 °C. At 770 °C ethanol conversion was complete, as shown in Fig. 4. In the temperature range from 520 to 620 °C, in which the ethanol conversion was almost constant, the products distribution changes (Table 2) evidencing that at these conditions occurred mass transfer limitations in gas phase.

The carbon-based products selectivities are mainly methane and CO, possibly due to acetaldehyde decomposition reaction that is favored on cobalt-based catalysts. The literature [20] reports that for temperatures higher than 500 °C, CO and methane selectivity gradually increase with temperature, as can be seen in Table 2. On the other hand, there is a clearly decrease in the amount of CO_2 formation, indicating that the reverse water–gas shift reaction favored CO formation (Eq. (6)). Moreover, according to the stoichiometry of the ethanol decomposition reaction, the H_2:CH_4 molar ratio must be equal to one. However, the methane selectivity was lower than H_2, suggesting that the steam reforming reaction of methane occurred simultaneously (Eq. (7)), contributing to a significant increase in the H_2 selectivity.

$$CH_{4(g)} + H_2O_{(s)} \rightarrow 3H_{2(g)} + CO_{(g)} \quad (7)$$

Ethyl ether formation was only observed at low temperatures, in which ethanol dehydration reaction is favored. At temperatures higher than 520 °C, the ethyl ether formation was not observed. Ethylene formation decreased as temperature increased, remaining at a constant value that disagrees with the literature [20]. Sahoo et al. [20] did not observe ethylene formation at temperatures higher than 400 °C.

3.2.2. Effect of O_2:ethanol molar ratio

The stoichiometry of the partial oxidation reaction implies that 0.5 mole of oxygen per mole of ethanol is required to produce CO

Table 2
Response of CO_2:CO molar ratio and products distribution during partial oxidation of ethanol at high temperatures (GHSV = $1{,}8 \times 10^4\ h^{-1}$; O_2:ethanol = 0.3).

T (°C)	$X_{Ethanol}$ (%)	CO_2/CO (molar ratio)	Selectivity (mol.%)					
			H_2	CH_4	CO	CO_2	Ethylene	Acetaldehyde
520	51.5	0.4	10.3	7.9	14.2	5.7	8.4	52.6
570	58.8	0.3	14.1	13.1	20.5	5.6	4.4	41.7
620	55.7	0.2	18.8	17.9	28.9	6.2	7.1	18.4
670	62.8	0.1	18.6	19.3	33.0	4.4	6.8	15.4
720	78.8	0.1	20.6	21.9	34.8	3.2	7.1	9.9
770	97.6	0.1	27.6	21.9	37.5	2.9	6.3	1.8

Table 3
Conversion of ethanol and products distribution on partial oxidation of ethanol at different O_2:ethanol molar ratios and constant T (420 °C).

O_2:ethanol (molar ratio)	$X_{Ethanol}$ (%)	CO_2:CO (molar ratio)	Selectivity (mol.%)						
			H_2	CH_4	CO	CO_2	Ethylene	Acetaldehyde	Ethyl ether
0.0	42.3	2.0	3.8	0.03	0.05	0.1	23.1	8.8	63.9
0.3	52.4	0.4	2.7	2.5	13.8	4.9	13.0	50.3	12.5
0.5	71.8	0.5	4.5	2.8	14.9	7.2	19.6	41.8	8.9
0.8	83.5	1.3	14.2	1.6	11.0	13.7	26.0	29.1	4.3

and H_2. The effect of this ratio was examined by varying the relative concentrations of O_2 and N_2 in the feed while maintaining the ethanol and total flows constant at 420 °C. Because O_2 is the stoichiometrically limiting reactant, ethanol conversion increased as the O_2:ethanol ratio increased from 0.3 to 0.8, as shown in Table 3.

According to the literature [22], cobalt catalysts are active in the dehydrogenation of ethanol to acetaldehyde and then in the steam reforming of acetaldehyde. The results presented by Pereira et al. [22] showed that the cobalt oxide, which is responsible for catalytic activation in the dehydrogenation of ethanol, is reduced to metallic cobalt under reaction conditions, which then carries out steam reforming of ethanol and acetaldehyde. However, in oxygen atmosphere the cobalt particles at the surface would oxidize favoring acetaldehyde production, avoiding its reformation under conditions of oxidative steam reforming.

In a deficient oxygen atmosphere, Co_3O_4/γ–Al_2O_3/cordierite catalyst promotes the dehydration of ethanol producing ethylene and ethyl ether, as expected. The literature [21] provides evidence that alumina support contains acidic sites that favor ethylene and ethyl ether formation, therefore could result in coke deposition.

The addition of oxygen to ethanol reactant feed affects significantly the pathway of reaction. The amount of ethylene and ethyl ether decreased as acetaldehyde became the main carbon content product. CO and CO_2 selectivity increased with oxygen addition, while CH_4 selectivity did not reach significant values. These results suggest that the oxygen addition favors water–gas shift reaction (Eq. (6)) and methane steam reforming (Eq. (7)), increasing CO_2 and hydrogen selectivity.

The results presented in Table 3 suggest that the monolithic catalyst structure facilitates the reactions of decomposition in the gas phase to form radicals that could be easily decomposed at low temperatures on the surface of the Co_3O_4/γ–Al_2O_3/cordierite catalyst.

3.2.3. Effect of hydrogen addition

To verify whether H_2 produced during the partial oxidation reaction was consumed for the formation of ethane and methane or the catalyst was reduced during the reaction, H_2 was added to the feed mixture at different H_2:ethanol molar ratio. The O_2:ethanol molar ratio was constant at 0.3 while the total flow rate was remained constant at 0.093 g s cm^{-3}. The results are presented in Table 4.

The amount of H_2 in the reactor output was determined and remained constant during the reaction process and equal to the feed gas composition. It shows that the hydrogen produced via ethanol partial oxidation reaction was not consumed to reduce the catalytic system. Furthermore, it also suggests that the cobalt active phase is present in its metallic form throughout all experiments.

As shown in Table 4, by increasing the H_2:ethanol molar ratio in the feed from 0 to 2 decreased ethanol conversion leading to a systematic increasing in the CO_2:CO molar ratio. Ethylene hydrogenation was not observed since ethane selectivity remained constant around 1.0%. The water–gas shift reverse reaction was not favored because a progressive increasing in the H_2 formation was not observed.

The fact that with decreasing of ethanol conversion we observed significant decreasing of ethylene and CO selectivity and increasing of CO_2 selectivity, it is possible to suggest that H_2 addition in the feed promotes indirectly the carbon deposition on the Co_3O_4/γ–Al_2O_3/cordierite surface catalyst through Boudouard reaction (Eq. (8)).

$$2CO(g) \rightleftarrows CO_2(g) + C(s) \quad (8)$$

Besides, ethylene decomposition could occur simultaneously. Taking into account that Co_3O_4 is not a reductive oxide, the carbon deposition could cause the deactivation of the catalyst.

3.2.4. Effect of water addition

The stoichiometry of the steam reforming reaction of ethanol implies that 3 moles of water per mole of ethanol is required to produce CO_2 and H_2, and less than 2 moles of water is required for the oxidative reforming [11]. To evaluate the water presence in the feed, ethanol (P. A.) was replaced by 95 vol.% hydrated ethanol. The H_2O:ethanol molar ratio remained constant at 0.2. The O_2:ethanol molar ratio increased from 0.3 to 0.8 while the total flow rate remained at 0.093 g s cm^{-3}. The results at 420 °C are presented in Table 5.

In a deficient oxygen atmosphere, the hydrated ethanol presented low conversion and the mainly products were H_2 and acetaldehyde. These results are expected since the Co_3O_4/γ–Al_2O_3 is active for dehydrogenation of ethanol. The presence of H_2O in the feed increased H_2 selectivity as the H atoms in the ethanol and water molecules can be converted into hydrogen [14]. Moreover, the high CO_2:CO molar ratio suggests that the water–gas shift reverse reaction was favored (Eq. (6)).

The addition of O_2 to hydrated ethanol reactant feed promoted the oxidative dehydrogenation reaction (Eq. (9)), increasing ethanol conversion while the acetaldehyde selectivity remained constant. The CO_2:CO molar ratio was close to 1.0, suggesting that

Table 4
Conversion of ethanol and products distribution on partial oxidation of ethanol at different O_2:ethanol molar ratios and constant T (420 °C).

H_2:ethanol (molar ratio)	$X_{Ethanol}$ (%)	CO_2:CO (molar ratio)	Selectivity (mol.%)					
			CH_4	CO	CO_2	Ethylene	Acetaldehyde	Ethyl ether
0.0	52.4	0.4	2.6	14.2	5.0	13.4	51.7	12.8
1.0	33.1	2.9	1.9	8.9	25.6	9.2	31.6	20.6
2.0	28.4	3.4	2.4	6.6	22.4	3.7	55.2	8.8

Table 5
Conversion of ethanol and products distribution on partial oxidation of hydrated ethanol at different O_2:ethanol molar ratios and constant T (420° C).

O_2:ethanol (molar ratio)	$X_{Ethanol}$ (%)	CO_2:CO (molar ratio)	Selectivity (mol. %)						
			H_2	CH_4	CO	CO_2	Ethylene	Acetaldehyde	Ethyl ether
0.0	2.6	2.8	23.2	0.6	1.1	3.1	8.5	50.5	12.5
0.3	45.2	1.0	5.6	4.2	12.7	12.1	8.3	50.6	6.1
0.5	61.8	0.8	9.8	5.1	15.6	11.7	8.5	47.3	1.4
0.8	78.5	0.5	19.9	8.7	18.9	9.8	4.2	38.1	0.0

the water–gas shift reaction equilibrium was achieved (Eq. (6)) limiting the amount of H_2 production.

$$CH_3CH_2OH_{(s)} \rightarrow CH_3CHO_{(l)} + H_{2(g)} \quad (9)$$

At O_2:ethanol molar ratio of 0.8, a significant modification in the products distribution was observed. The presence of larger amount of O_2 increased the selectivity of H_2 and CO, but decreased the selectivity of acetaldehyde. In this case, the amount of radicals was increasing, which are reformed by steam at the cobalt surface.

The literature [21] reports that low ratios of water and ethanol may increase the hydrogen selectivity on cobalt catalyst, since water–gas shift reaction (Eq. (6)) and steam reforming of methane equilibrium are favored with increasing water concentration in the feed.

3.2.5. Catalyst stability

Before the stability test, the Co_3O_4/γ–Al_2O_3/cordierite catalyst was run on stream during 30 days at different reaction temperatures varying from 260 to 620 °C and oxygen–to–ethanol ratio varying from 0.3 to 0.8. Then, it was submitted to a stability test for 30 h at a constant temperature reaction of 420 °C, a volumetric flow rate at 0.093 g s cm^{-3} and O_2:ethanol molar ratio of 0.3.

Fig. 5 shows the ethanol conversion with time-on-stream. No signs of catalyst deactivation were observed. A small activation occurred in the first 600 min, however, it was very stable for 30 h on stream. It is significant to note the fact that the distribution of products (not shown here) was not altered with time-on-stream and also constant.

The ethanol conversion may occur in two parallel reaction routes. First, ethanol is dehydrogenated to produce acetaldehyde, which is decomposed following the steam reforming of methane. Secondly, dehydration of ethanol to produce ethylene, which is decomposed by breaking the C–C bond, that is responsible for coke deposition. In this context, the cobalt-based catalysts, such as Co/Al_2O_3, Co/SiO_2, Co/MgO and Co/$SrTiO_3$, are active and selective for steam reforming of ethanol. However, these catalysts have the disadvantage of deactivating with coke deposition through the ability of cobalt to break the C–C bonds [30].

Catalysts deactivation may be attributed to the surface coating with carbon. This carbon layer hinders the contact between the gas phase and the active sites [31]. Although there was no apparent catalyst deactivation, a large amount of carbon formation was observed at the end of the experiments. The specific weights of coke or carbon deposition on catalyst surface can be obtained from TG results, which represented a weight increase of 89% on the catalyst weight. Fig. 6 shows the DTA and TG results of used Co_3O_4/γ–Al_2O_3/cordierite. The exothermic peaks in DTA curve should be attributed to the combustion of coke deposited and the peaks at different temperatures related with different properties of coke. Amorphous structures composed of large particles or aggregate materials are characterized as stable and could decompose at high temperatures [32].

Between 400 and 600 °C, it is possible to see a weight loss of 79%, corresponding to exothermic peaks around 500 °C and with lower intensity at 650 °C. These results suggest that a large amount of carbon deposited at the surface is reactive, characteristic of a carbon structure less stable, such as filamentous structure.

The exothermic peak at 650 °C could be attributed to the presence of carbon graphite. Since there was no sign of catalyst deactivation, it is possible to say that the small amount of carbon graphite, approximately 10%, was not able to decrease catalyst performance. Furthermore, these results suggest that most of the cobalt particles are encapsulated by structures of filamentous carbon. In this case, the carbon deposited is transformed to fiber-like carbons, which stretch away from catalyst particles, and thus the deactivation was not sensitive [30].

After the long-term stability experiments this catalyst was submitted for textural analysis. The catalyst deteriorates and crumbles, turning to a black powder at the end of all experiments. This material was analyzed by Raman spectroscopy. Fig. 7 shows

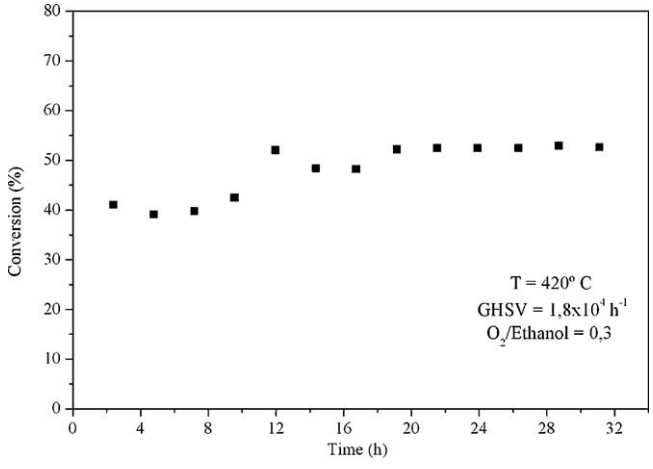

Fig. 5. Conversion of ethanol on partial oxidation of ethanol as function of time on stream (hour).

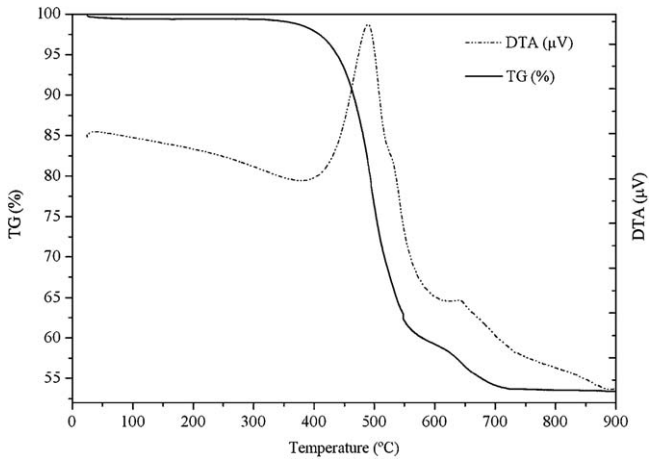

Fig. 6. DTA-TG results of used Co_3O_4/γ–Al_2O_3/cordierite catalyst.

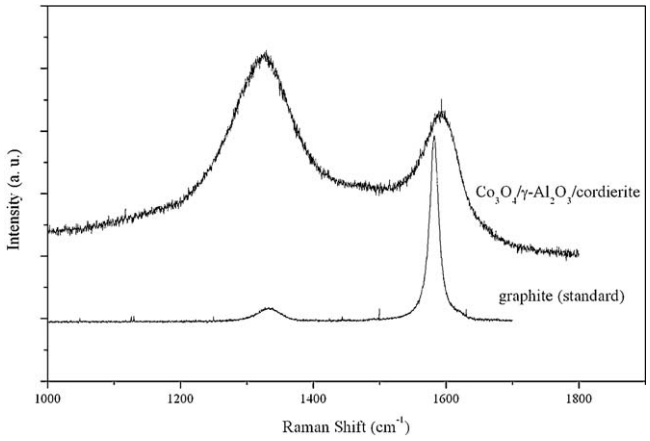

Fig. 7. Raman spectrum of used Co_3O_4/γ–Al_2O_3/cordierite catalyst.

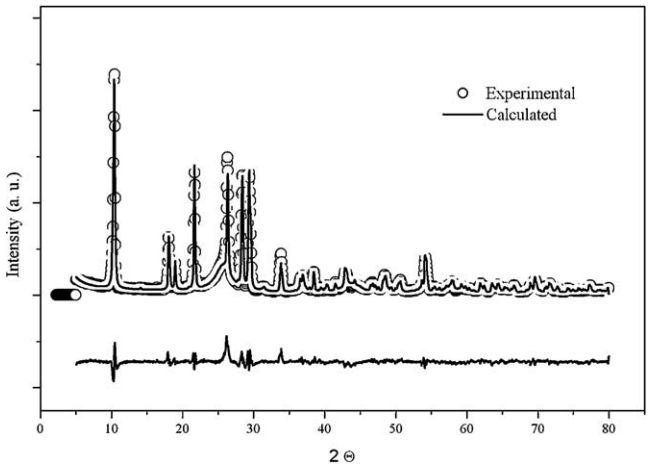

Fig. 8. Diffraction pattern of used Co_3O_4/γ–Al_2O_3/cordierite catalyst. Open circles: experimental; solid line: calculated; bottom line: difference between observed and calculated diagrams.

the Raman spectra of Co_3O_4/γ–Al_2O_3/cordierite after the experiments, which exhibited two bands in the 1300–1600 cm^{-1} region, corresponding to carbon deposits. The two bands that can be assigned to the D and G lines are centered at 1300 and 1600 cm^{-1}, respectively.

According to the literature [22,33], D band (1300 cm^{-1}) is assigned to the defects and impurities present in carbon nanofibers while G (1600 cm^{-1}) band is assigned to the stretching mode of the C–C bound in the graphite plane. The relative intensity of D and G bands (I_D/I_G) indicates the degree of graphitization of the carbon deposited on the catalyst surface. The relative intensity between the G and D bands was found to be 1.2 for Co_3O_4/γ–Al_2O_3/cordierite, suggesting that the carbon formed on this surface has a defective structure.

X-ray diffraction was done to verify possible changes in crystalline structure of Co_3O_4/γ–Al_2O_3/cordierite after the partial oxidation of ethanol. In Fig. 8 is presented the diffratogram for a used sample and the pattern obtained by refinement calculation. The calculated pattern was obtained using the whole pattern refinement program FULLPROF 4.4 [34], using the Rietveld method [35] assuming the presence of cordierite, Co_3O_4 and carbon, based on literature reports for the three phases respectively [36–38].

The diffraction pattern in Fig. 8 is dominated by the diffraction peaks assigned to cordierite crystalline phase. The diffraction peaks at approximately 19, 31, 38 and 44 in the 2θ scale are assigned to cobalt oxide, which accounts for 6.0 wt.% of the total catalyst weight. No loss of active phase was observed after a long period of exposure to the experimental conditions.

The comparison of experimental and the calculated diffraction patterns showed a great difference in the diffraction peak of carbon, as a result of the approximation done, taking into account the parameters from graphite that only enables to quantify the carbon deposited, but it is impossible to identify the nature of carbon. In this sample, a high amount of carbon was observed, which accounts for 33 wt.%.

It is expected that cobalt-based catalyst after exposure to high temperatures should react with Al_2O_3 and SiO_2 present in the cordierite structure. The MgO active sites are also susceptible to cobalt attack. However, according to Fig. 8, there is no evidence that cobalt had reacted with the support causing its degradation. Based on the X-ray diffraction results, it is possible to say that the Co_3O_4/γ–Al_2O_3/cordierite was crumbled owing to mechanical stress caused by carbon filaments growth.

Similar results were found in the literature [31] and these results showed, comparing the diffraction pattern of new and the used catalyst, that after the experiments, the main change that may occur on account of disproportionation of CO reaction with a CO–CO_2–H_2 or CO–CO_2 mixture was the appearance of new peaks assigned to carbon. It is relevant to mention here that the cobalt phase did not change, although the experiments were performed until complete deactivation of the catalyst.

The experiments with hydrated ethanol on Co_3O_4/γ–Al_2O_3/cordierite catalyst were performed at 420 °C, O_2:ethanol ratio of 0.3 to 0.8 and 0.093 g s cm^{-3} total volumetric flows. After reaction,

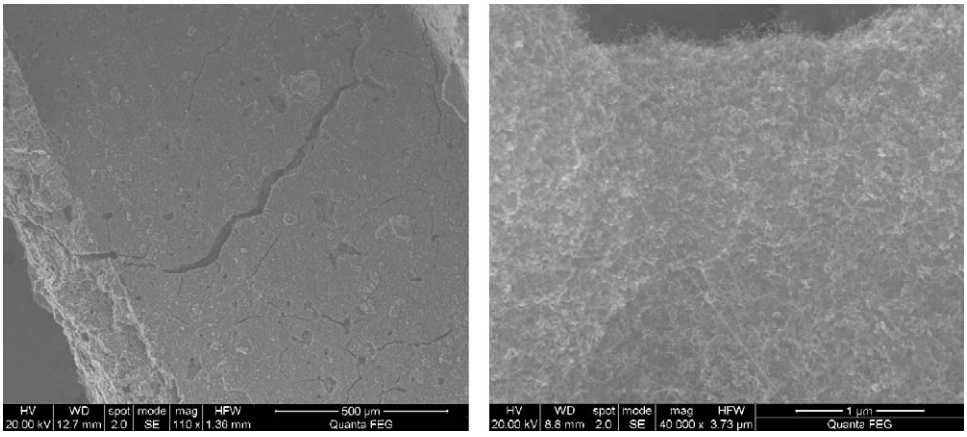

Fig. 9. SEM Images of Co_3O_4/γ–Al_2O_3/cordierite after partial oxidation of hydrated ethanol reaction: details of catalyst surface.

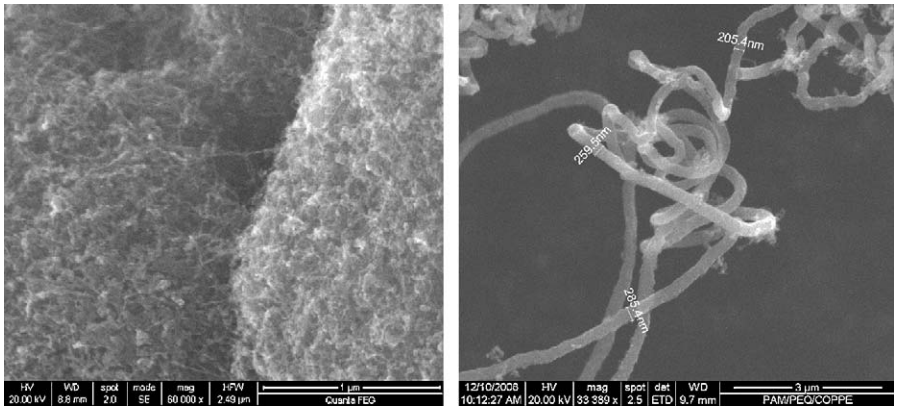

Fig. 10. SEM Images of Co_3O_4/γ–Al_2O_3/cordierite after partial oxidation of hydrated ethanol reaction: formation of carbon filaments inside the crack.

the catalyst showed signs of degradation and a fragile and brittle structure. Images of scanning electron microscopy in field emission (FEG-SEM) of the catalyst surface confirmed the presence of structured carbon, suggesting that carbon filament growth is responsible for the monolithic structure degradation.

The literature [30] reports that at temperatures higher than 500 °C coke could be transformed to carbon filament during steam reforming reaction of ethanol on Co–CeO_2 catalyst. This filament stretches away from the catalyst particle, thus the encapsulation of catalyst particle is much lighter and no layered coke is observed. So, at temperatures between 500 and 550 °C, the catalyst deactivation becomes insignificant, even forming a large amount of non-carbon graphite.

FEG-SEM images of Co_3O_4/γ–Al_2O_3/cordierite catalyst in Fig. 9 show the surface of catalyst with few cracks after reaction experiment. It is seen from the magnified picture of 40 k that a layer of fiber-like carbons was formed overall catalyst surface. Measurements of EDS (not shown here) confirm this observation.

Fig. 10 shows details of the fiber-like carbons layer inside the crack of catalyst surface. It is seen from the magnified picture of 60 k that carbon particles clumped together into nanofiber ropes, which seem to be thicker and long. Detail of a nanofiber rope formed is seen in Fig. 10, which presents typical morphologic characteristic of carbon nanofibers, such as very sinuous and defective structures with tube diameters about 200 nm.

4. Conclusions

The partial oxidation of ethanol was studied using a Co_3O_4/γ–Al_2O_3/cordierite structured catalyst. This structure of parallel channels favors the reactions that occur in gas phase, presenting in some conditions of temperature and flow rate effects of mass transfer in gaseous film. On this catalyst, acetaldehyde was the main product constituted of carbon in the reaction of ethanol partial oxidation. However, at high temperatures and O_2–to–ethanol ratios this catalyst favored the decomposition reaction in gas phase, obtaining low values for methane selectivity. These results confirm the cobalt ability to promote steam reforming reaction to improve H_2 selectivity. Applying hydrated ethanol in the partial oxidation reaction on Co_3O_4/γ–Al_2O_3/cordierite catalyst increased H_2 selectivity too. The presence of water in the ethanol feed allowed the occurrence of the steam reforming reaction on the catalyst surface. The low CO_2:CO ratio observed in most experiments indicates that the inverse gas-shift reaction favored CO formation in gas phase decreasing H_2 selectivity, as well as limited its formation.

Acknowledgements

The authors would like to acknowledge CNPq for the financial support. One of the authors (Clarissa P. Rodrigues) would like to thank Eka Chemicals Brazil S./A. for the EKA-SOL product donation.

References

[1] D.A. Hickman, L.D. Schmidt, J. Catal. 138 (1992) 267–282.
[2] D.A. Hickman, E.A. Hampfear, L.D. Schmidt, Catal. Lett. 17 (1993) 223–237.
[3] S.S. Bharadwaj, L.D. Schmidt, Fuel Process. Technol. 12 (1995) 109–127.
[4] A.G. Dietz III, A.F. Carlsson, L.D. Schmidt, J. Catal. 176 (1996) 459–473.
[5] K.L. Hohn, L.D. Schmidt, Appl. Catal. A 211 (2001) 53–68.
[6] J.J. Krummenacher, L.D. Schmidt, J. Catal. 222 (2004) 429–438.
[7] L.D. Schmidt, E.J. Klein, C.A. Leclerc, J.J. Krummenacher, K.N. West, Chem. Eng. Sci. 53 (2003) 1037–1041.
[8] A. Cybulski, J.A. Moulijn, Structured Catalysis and Reactors, Taylor & Francis, 2006
[9] G. Groppi, A. Beretta, E. Tronconi, in: A. Cybulski, J.A. Moulijn (Eds.), Structured Catalyisis and Reactors, Taylor & Francis, 2006, pp. 243–310.
[10] S. Cavallaro, V. Chiodo, S. Freni, N. Mondello, F. Frusteri, Appl. Catal. A: General 249 (2003) 119–128.
[11] J.R. Salge, G.A. Deluga, L.D. Schmidt, J. Catal. 235 (2005) 69–78.
[12] D.K. Liguras, K. Goudani, X.E. Verykios, J. Hydrog. Energy 29 (2004) 419–427.
[13] D.K. Liguras, K. Goudani, X.E. Verykios, J. Power Sources 130 (2004) 30–37.
[14] G.A. Deluga, J.R. Salge, L.D. Schmidt, X.E. Verykios, Science 303 (2004) 993–997.
[15] L. Mattos, F. Noronha, J. Power Sources 152 (2005) 50–59.
[16] A.N. Fatsikostas, D.I. Kondarides, X.E. Verykios, Catal. Today 75 (2002) 145–155.
[17] A.N. Pestryakov, V.V. Lunin, A.N. Devochkin, L.A. Petrov, N.E. Bogdanchikova, V.P. Petranovskii, Appl. Catal. A 227 (2002) 125–130.
[18] E.C. Wanat, B. Suman, L.D. Schmidt, J. Catal. 235 (2005) 18–27.
[19] A. Casanovas, C. de Leitenburg, A. Trovarelli, J. Llorca, Catal. Today 138 (2008) 187–192.
[20] D.R. Sahoo, S. Vajpai, S. Patel, K.K. Pant, Chem. Eng. J. 125 (2007) 139–147.
[21] H. Song, L. Zhang, R.B. Watson, et al. Catal. Today 129 (2007) 346–354.
[22] E.B. Pereira, N. Homs, S. Martí, et al. J. Catal. 257 (2008) 206–214.
[23] G. Saracco, L. Montanaro, Ind. Eng. Chem. Res 34 (1995) 1471–1479.
[24] X. Wu, D. Weng, S. Zhao, W. Chen, Surf. Coat. Technol. 190 (2005) 434–439.
[25] M. Valentini, G. Groppi, C. Cristiani, M. Levi, E. Tronconi, P. Forzatti, Catal. Today 69 (2001) 307–314.
[26] H.S. Fogler, Elementos de Engenharia das Reações Químicas, LTC Editora, Rio de Janeiro, 2002.
[27] C.P. Rodrigues, V. Teixeira da Silva, M. Schmal, Catal. Commun. 10 (2009) 1697–1701.
[28] F. Haga, T. Nakajima, K. Yamashita, et al. React. Kinet. Catal. Lett 63 (1998) 253–259.
[29] G. Jacobs, R.A. Keogh, B.H. Davis, J. Catal. 245 (2007) 326–337.
[30] H. Wang, Y. Liu, et al. Chem. Eng. J. 145 (2008) 25–31.
[31] J.P. Pinheiro, M.C. Schouler, E. Dooryhee, Solid State Commun. 123 (2002) 161–166.
[32] A.W. Musumeci, G.G. Silva, W.N. Martens, et al. J. Therm. Anal. Calorim. 88 (3) (2007) 885–891.
[33] E. Dervishi, Z. Li, A.R. Biris, D. Lupu, S. Trigwell, A.S. Biris, Chem. Mater. 19 (2007) 179–184.
[34] J. Rodriguez-Carvajal, 2009, Short reference guide of the program FULLPROF, disponível em http://www.ill.eu/sites/fullprof, visitado em fevereiro/2009.
[35] H.M. Rietveld, J. Appl. Crystallogr. 2 (2) (1969) 65–71.
[36] M.F. Hochella, G.E. Brown, et al. Phys. Chem. Miner. 64 (1979) 337–351.
[37] X. Liu, C.T. Prewitt, Phys. Chem. Miner. 17 (1990) 168–172.
[38] P. Trucano, R. Chen, Nature 258 (1975) 136–137.